Journal of Advanced Research 24 (2020) 251–259

Contents lists available at ScienceDirect

Journal of Advanced Research

journal homepage: www.elsevier.com/locate/jare

Synthetic bulky NS4A peptide variants bind to and inhibit HCV NS3 protease

Moustafa E. El-Araby [a,*], Abdelsattar M. Omar [a,b], Sameh H. Soror [c,d], Stefan T. Arold [e], Maan T. Khayat [a], Hani Z. Asfour [f], Faida Bamane [g], Mahmoud A. Elfaky [h]

[a] Department of Pharmaceutical Chemistry, Faculty of Pharmacy, King Abdulaziz University, Alsulaymanyah, Jeddah 21589, Saudi Arabia
[b] Department of Pharmaceutical Chemistry, Faculty of Pharmacy, Al-Azhar University, Cairo 11884, Egypt
[c] Department of Biochemistry and Molecular Biology, Faculty of Pharmacy, Helwan University, Ain Helwan, P.O. 11795, Cairo, Egypt
[d] Center for Scientific Excellence Helwan Structural Biology Research (HSBR), Faculty of Pharmacy, Helwan University, Ain Helwan, P.O. 11795, Cairo, Egypt
[e] King Abdullah University of Science and Technology, Computational Bioscience Research Center, Division of Biological and Environmental Sciences and Engineering, Thuwal 23955-6900, Saudi Arabia
[f] Department of Medical Microbiology and Parasitology, Faculty of Medicine, King Abdulaziz University, Jeddah 21589, Saudi Arabia
[g] Department of Biochemistry, Faculty of Medicine, King Abdulaziz University, Jeddah 21589, Saudi Arabia
[h] Department of Natural Products and Alternative Medicine, Faculty of Pharmacy, King Abdulaziz University, Alsulaymanyah, Jeddah 21589, Saudi Arabia

GRAPHICAL ABSTRACT

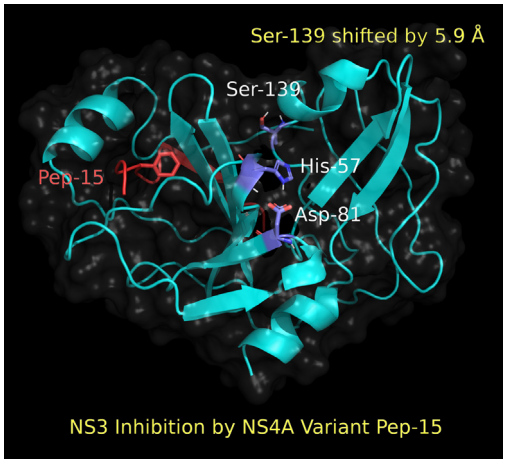

ARTICLE INFO

Article history:
Received 8 September 2019
Revised 3 November 2019
Accepted 2 January 2020
Available online 3 January 2020

Keywords:
DSLS

ABSTRACT

NS4A is a non-structural multi-tasking small peptide that is essential for HCV maturation and replication. The central odd-numbered hydrophobic residues of NS4A (Val-23‘ to Leu-31‘)[i] are essential for activating NS3 upon NS3/4A protease complex formation. This study aims to design new specific allosteric NS3/4A protease inhibitors by mutating Val-23‘, Ile-25‘, and Ile-29‘ into bulkier amino acids. Pep-15, a synthetic peptide, showed higher binding affinity towards HCV-NS3 subtype-4 than native NS4A. The K_d of Pep-15 (80.0 ± 8.0 nM) was twice as high as that of native NS4A (169 ± 37 nM). The mutant Pep-15 inhibited the catalytic activity of HCV-NS3 by forming an inactive complex. Molecular dynamics simulations suggested that a cascade of conformational changes occurred, especially in the catalytic triad arrangements,

Peer review under responsibility of Cairo University.
* Corresponding author.
E-mail address: madaoud@kau.edu.sa (M.E. El-Araby).
[i] The prime symbol (‘) is used to distinguish between NS4A residues and NS3 residues of (no prime).

https://doi.org/10.1016/j.jare.2020.01.003
2090-1232/

Fluorescence anisotropy
Allosteric inhibitor
HCV
NS3/4A
Peptide mutants

thereby inactivating NS3. A large shift in the position of Ser-139 was observed, leading to loss of critical hydrogen bonding with His-57. Even though this study is not a classic drug discovery study—nor do we propose Pep-15 as a drug candidate—it serves as a stepping stone towards developing a potent inhibitor of hitherto untargeted HCV subtypes.

Introduction

Hepacivirus, *Flavivirus*, *Pestivirus*, and *Pegivirus* are the four genera of viruses belonging to the *Flaviviridae* family that have been discovered to date [1–3]. This family includes dangerous human pathogens that pose worldwide health risks, such as hepatitis C virus (HCV), dengue virus, yellow fever virus, Japanese encephalitis virus, West Nile virus, and Zika virus (https://www.cdc.gov/vhf/virus-families/flaviviridae.html). All *Flaviviridae* have a single-stranded, non-segmented RNA genomes that encode for a single, non-functional polyprotic chain [4]. This viral polyprotein is processed into several structural and non-structural/functional proteins upon cleavage by viral and host proteases [4,5]. NS4A is a small peptide commonly encoded in all *Flaviviridae* family and considered as essential non-structural protein for replication, though its role is not the same among these viruses [4]. In hepatitis C virus (HCV), the non-structural protein NS4A is a small hydrophobic peptide (54 amino acid) with multiple functions. NS4A is a necessary component not only for the activation of NS3 (both protease and RNA-helicase domains) [6,7] but also for its integration to the host cell's endoplasmic reticulum [8]. In addition, NS3/4A helps the virus in evading the host immune response to the viral invasion *via* cleavage and inactivation of CARDIF and TRIF, two critical sensing proteins that trigger antiviral responses [9,10]. To accomplish its assembly-assistant role, NS4A's hydrophobic N-terminal residues (21'-34') intercalate between the A_0 and A_1 β-sheets at the N-terminal of the NS3 apoprotein to form an active protease [11,12]. This assembly brings the NS3 N-terminal together and rearranges the apoprotein into an α-helix (residues 13–22) and a β-strand (A_0 sheet, residues 2–10). Structural studies have provided evidence that NS4A binding optimizes the distances of the catalytic triad (His-57/Asp-81/Ser-139) to bolster the catalytic activities of NS3 by approximately 950 fold [13]. Several studies have reported that the central hydrophobic region (residues 21'–32') of NS4A is sufficient for NS3 *in vitro* protease activation [11,14-18]. Furthermore, serine and alanine scanning have revealed that the odd-numbered hydrophobic residues Val-23', Ile-25', Gly-27', Ile-29', and Leu-31', but not the even-numbered residues in the sequence, are crucial for the enzyme activation [16]. In fact, following the identification of NS3/4A protease as a target to develop HCV antiviral agents, the NS4A binding site has been proposed as a target for allosteric NS3 inhibitors. Without much of experimental corroboration, it has been postulated that a competitive ligand for this site might alter the structure of NS3 and the conformation of the active site sufficiently, leading to an inactive enzyme [19]. For instance, Kim et al reported crystal structure of NS3/4A complex and detailed features of NS4A binding. In conclusion, they suggested that this site should be considered as a suitable target to develop NS3 inhibitors [11]. Similar theoretical arguments were provided in other studies that were directed to specifying the NS4A residues involved in binding with NS3 protease [14,17]. In another study, also directed to determination of important NS4A residues, it was found that replacing the positively charged Arg-28 residue by a neutral Gln produced an inhibitor of NS3 that binds to the NS4A pocket [16]. Three years later, De Francesco et al argued against this approach because "The interaction between NS3 and NS4A involves a very large surface area and therefore it is not a likely target for the development of inhibitors" [20]. Interestingly, Kim et al used similar argument against the NS3/4A substrate site as they characterized it as shallow, solvent accessible and has large surface area [11]. Their theory was conflicted by successful development of substrate-site peptidomimetic inhibitors of NS3/4A as the first approved class of HCV direct antiviral agents (DAAs) [21]. Because of conflicting information and because one inhibitor example (Arg-NS4A-Gln) cannot be considered enough evidence to make conclusion in favor or against the concept of NS4A site inhibitors, we decided to investigate this approach with NS4A synthetic peptide analogues in a systematic and conclusive work. Our hypothesis was that mutating certain residues (Val-23', Ile-25', and Ile-29') in HCV-NS4A to bulkier amino acids should be able to bind in higher affinity than the native NS4A but inactivate this enzyme. The success of these peptides to replace the native NS4A and inhibit the enzyme was envisioned to pave the way to design non-peptide HCV NS4A binding site inhibitors and possibly, other related viruses of *Falviviridae*. A good example to follow was the development of HCV NS3/4A substrate site inhibitors, which was coined subsequent to studies on synthetic peptide substrate analogues [22–24] and later evolved to non-peptide small molecule DAAs [21,25]. Accordingly, synthetic peptide inhibitors are suitable, by scientific principles, to validate the approach, gain information about structure-activity relationships and set forth protocols of enzymatic assays. We were also determined to focus primarily on testing variable size mutants, investigate their binding affinity, competition potency and inhibition of HCV NS3 as the scope of our study.

Material and methods

Material and reagents

Unless mentioned otherwise, all chemicals were of molecular biology grade and purchased from Sigma Aldrich (St Louis, MO, USA).

NS4A wild type and mutants

NS4A wild type, mutants, and fluorescein isothiocyanate-NS4A (FITC-NS4A) synthetic peptides were ordered from GenScript (Hong Kong). Synthetic NS4A mutant peptides (Table 1) were ordered from Biosynthesis (Lewisville, TX, USA). All synthetic peptides used in this study contained Lys-Lys (KK) termini to increase aqueous solubility; moreover, the synthetic peptides possessed a purity of 85% or higher (LC/MS).

NS3 construct

A synthetic gene coding for the NS3 domain of HCV genotype-4 (HCV-4) [26], the most abundant HCV in Saudi Arabia and Egypt [27,28], was synthesized by GenScript (Hong Kong); moreover, the nucleotide sequence was optimized for *E. coli* codon usage. The synthetic gene fragment *Nde*I-*Bam*HI was cloned into the expression vector pET-3a (Novagen-Merck KGaA, Darmstadt, Germany). The resulting construct was sequenced to confirm that the clone containing the gene is in the correct frame.

Table 1
Structure of native and mutant NS4A used in this study. The structures of the unnatural *S*-amino acids xG and hI are illustrated in Fig. 1.

Code	Structure	Type of mutation
NS4A	$GSV_{23}VI_{25}VGRI_{29}VLSG$	Native
Pep-1	GSVVIVGR**F_{29}**VLSG	Ile-29
Pep-2	GSVVIVGR**W_{29}**VLSG	
Pep-3	GSVVIVGR**A_{29}**VLSG	
Pep-4	GSVVIVGR**hI_{29}**VLSG	
Pep-5	GSVVIVGR**xG_{29}**VLSG	
Pep-6	GSVV**F_{25}**VGRIVLSG	Ile-25
Pep-7	GSVV**W_{25}**VGRIVLSG	
Pep-8	GSVV**A_{25}**VGRIVLSG	
Pep-9	GSVV**hI_{25}**VGRIVLSG	
Pep-10	GSVV**xG_{25}**VGRIVLSG	
Pep-11	GS**F_{23}**VIVGRIVLSG	Val-23
Pep-12	GS**W_{23}**VIVGRIVLSG	
Pep-13	GS**A_{23}**VIVGRIVLSG	
Pep-14	GS**hI_{23}**VIVGRIVLSG	
Pep-15	GS**xG_{23}**VIVGRIVLSG	

Protein expression

The NS3 domain of HCV-4 was expressed in *E. coli* Rosetta (DE3) pLysS, according to standard procedures [11]. A synthetic gene coding for the NS3 domain was subcloned into the expression vector pET-3a. *E. coli* Rosetta (DE3) pLysS cells, freshly transformed with the pET-3a plasmid, were grown at 37 °C in luria bertani (LB) agar supplemented with 50 μg/mL ampicillin. In the process, 100 mL of bacterial culture in Luria Broth (LB) medium was grown overnight at 37 °C and used to inoculate 10 L of LB medium in a 14-liter fermenter flask (New Brunswick Scientific Co., CT, USA). The media was supplemented with ampicillin (50 μg/mL). The culture was grown until it reached an OD_{600} of 0.5–0.6, then it was cooled to 25 °C and 1 mM isopropyl-β-thiogalactoside (IPTG) was added. Proteins were expressed overnight, and the cells were harvested on the following day.

Protein purification

The proteins were purified using equilibrated nickel nitrilotriacetic acid (Ni-NTA) beads, and the poly-histidine tag was not removed. During the process, the cells were re-suspended (1 g/5 mL) in buffer (50 mM *N*-2-hydroxyethyl-piperazine-*N*′-2-ethanesulfonic acid [HEPES], 0.3 M NaCl, 10% glycerol, 2 mM β-mercaptoethanol, pH 8). Lysozyme was added (1 mg/mL) followed by a protease inhibitor cocktail tablet and the suspension was subsequently sonicated. The cellular lysate was centrifuged to collect the clear supernatant that contained the desired NS3 protein. The protein was then purified using pre-equilibrated Ni-NTA beads (Qiagen, USA). The beads were washed with buffer (50 mM HEPES, 0 3 M NaCl, 10% glycerol, 2 mM β-mercaptoethanol, 20 mM imidazole, pH 8) and eluted with another buffer (50 mM HEPES, 0.3 M NaCl, 10% glycerol, 2 mM β-mercaptoethanol, 350 mM imidazole, pH 8). Fractions were collected and concentrated using an Amicon Ultra-4 3000 MWCO centrifugal device (Millipore, Germany). Protein purity after Ni-affinity purification step was never less than 70%. The purity, as estimated by SDS-PAGE, was sufficient to perform all experiments described in this study; moreover the protein was stable for several hours during the test conditions [26].

When needed, further purification of the protein was carried out on Superdex 75 16/90 column (GE Healthcare, USA) equilibrated in buffer (20 mM HEPES, 10 mM Dithiothreitol [DTT], 200 mM NaCl, pH 7.6) and ran at rate of 1 mL/min, followed by SDS-PAGE for purity estimation (see Supplementary Material, Fig. S1).

Binding studies using differential static light scattering (DSLS)

We studied the binding capacity between NS4A and its mutants and NS3 by DSLS using Stargazer-2™ (Harbinger Biotechnology and Engineering Corporation, Toronto, Canada). This method assesses protein stability by monitoring aggregate formation by gradually elevating the temperature [29]. NS3 domain stability upon binding to NS4A was measured by monitoring denatured protein aggregation at 600 nm upon increasing the temperature from 25 to 85 °C (with 0.5 °C increments).

The NS3 domain (15 μM) (alone or mixed with specified molar equivalents of synthetic peptides) was added to the binding buffer (20 mM HEPES, 10 mM DTT, 200 mM NaCl, pH 7.6). The mixture was incubated at 23–25 ℃ with gentle shaking for a specified amount of time. Afterward, 10 μL of the mixture was transferred to a clear bottomed Nunc 384-well plate and covered with 10 μL of paraffin oil to minimize evaporation. Protein aggregation was monitored by tracking the changes in scattered light using a charged coupled device camera. Snapshot images of the plate were taken after every 0.5 °C increment. The pixel intensities in each preselected region of the wells were integrated using an image analysis domain impeded in Sargazer-AIR® software to generate a representative value of the total amount of scattered light in that region. The intensities were then plotted against temperature for each sample well, and fitted to obtain the aggregation temperature (T_{agg}). Aggregation was monitored and analyzed to assess the effect of NS4A and its synthetic analogs on the stability of NS3 as an indicator of binding.

Determination of the dissociation constant of NS4A

Fluorescence anisotropy was used to determine the numerical binding affinity (in terms of the dissociation constant [K_d]) of NS4A and its mutant Pep-15 (the synthetic mutant that showed higher affinity than the native NS4A in the previous DSLS, see Results and Discussion section below).

Serial dilutions of NS3 were prepared in a 96-well plate using a binding buffer (20 mM HEPES, 10 mM DTT, 200 mM NaCl, pH 7.6), 0.1 μM fluorescein isothiocyanate-labeled NS4A (FITC-NS4A) was added and shaken for 15, 45, 90 and 120 min at room temperature. A total of 20 μL of the mixture was then transferred to a black reading Nunc 384-well plate. Fluorescence was measured at 480/520 nm (excitation/emission) using a PHERAstar™ plate reader (BMG Labtech, Ortenberg, Germany). Emitted fluorescence was proportional to the concentration of the FITC-NS4A/NS3 complex (bound form).

Binding affinity, expressed as the dissociation constant (K_d) of NS4A, was calculated using the non-linear regression equation in GraphPad Prism v.7 software (La Jolla California USA), according to the following equation:

$$Y = B_{max} * X/(K_d + X)$$

where B_{max} is the maximum specific binding capacity in the same units as Y and was fitted to data to produce a K_d.

Pep-15 and FITC-NS4A competition assay

To measure the binding affinity of the mutant NS4A Pep-15, we designed a competition assay as follows: 1.8 μM NS3 and 0.1 μM FITC-NS4A were mixed and added to a serial dilution of Pep-15 ranging from 100 μM to 0.195 μM; then, fluorescence was measured under excitation/emission wavelengths of 480/520 nm.

The binding affinity expressed as the dissociation constant (K_d) of Pep-15, was determined by non-linear fitting of a single binding site using prism in GraphPad Prism v.8 software.

Enzyme inhibition assay

The assay was performed using SensoLyte-520® HCV Protease Assay Kit *Fluorometric* (Anaspec, Fremont, CA, USA), after modifying the procedure to suit the purpose of measuring allosteric inhibition. NS3 (4.0 μM) was mixed with Pep-15 (concentrations ranging from 0.001 to 50 μM) for 15 min. The kit contains a substrate peptide SLGRKIQIQ, which is derived from the NS4A/NS4B cleavage site. The substrate peptide was conjugated to 5-carboxyfluorescein (5-FAM) as a donor (fluorophore) and QXL™520 as an acceptor (quencher) [30]. The system is known as fluorescence resonance energy transfer (FRET). This FRET analysis was performed as instructed by the manual provided by the kit and fluorescence was monitored at 490/520 nm (excitation/emission).

Molecular modeling

Hardware and software

Molecular modeling experiments were performed using SYBYL-X v2.0 software package (licensed to the Faculty of Pharmacy, King Abdulaziz University) installed on a common desktop running Windows 7 operating system equipped with the Samsung SyncMaster 2233RZ 120 Hz LCD Display™ (3D ready) and the Nvidia GeForce 3D Vision Glasses Kit™. The images were generated using Pymol v. 2.3, free online software (https://pymol.org/2/).

Protein preparation

The 3-dimensional structure of the NS3/4A protease [18] was downloaded from the Protein Data Bank (https://rcsb.org, Code: 1NS3), and its dimeric structure was simplified to a monomer and optimized using SYBYL-X's tools (Biopolymer > Prepare Structure). The Pep-15 was prepared using Biopolymer > Composition > Mutate Structure tools.

Molecular mechanics

Molecular mechanics was performed using SYBYL-X's Staged Minimization tools (Force Field: Amber 7 FF02, Charges: Amber) [31].

Molecular dynamics (MD)

MD simulations were set on the following parameters: length = 2,000,000 fs, temperature = 310 K, snapshot every 5 fs, step 1 fs, max iterations = 100, non-bonded update very 25 fs, energy setup Amber 7 ff02 force field. Other parameters were used according to the default parameters given by Sybyl-X.

Results and Discussion

The rationale of the study

As mentioned above, when NS4A binds to the protease domain of NS3, it attains the form of a β-strand that intercalates the A_0 and A_1 β-strands at the N-terminal of the apoprotein. Based on crystallographic studies, NS4A appears as an extended strand, except for one backbone bond between α-carbon and the carbonyl of Val-26'. We noticed that this kink is conserved in the NS3/NS4A structures hosted on the Protein Data Bank (PDB) archive [11,32–34]. For instance, PDB code 1NS3 shows a *cis* bond with a nearly eclipsed dihedral angle of 14°, facilitated by the presence of Gly-27'. In context, this might explain why the Gly-27 sequence is necessary for binding and activating NS3 (for further details about NS4A conformations, see Supplementary Material, Figs. S2–S4). We concluded that peptides with mutations at Gly-27 should fail to bind and, therefore, we did not include those mutants in our study.

The even-numbered NS4A residues (Ser-22', Val-24', Val-26', Arg-28', Val-30', and Ser-32') were facing and interacting with the solvent-exposed A_0 sheet (residues Thr-4 to Gln-9) at the N-terminal of the NS3 protein. Conversely, odd-number NS4A residues (Val-23', Ile-25', Gly-27', Ile-29', and Leu-31') were facing inward, towards the A_1 sheet (residues Glu-58 to Ser-63), which is mostly buried within the protein's core [18]. Therefore, we hypothesized that certain bulkier hydrophobic mutated core residues (Val-23', Ile-25', and Ile-29') might be capable of binding; however, this binding occurs with induction of local conformational changes to their corresponding NS3 binding pockets, which could collectively affect the allosteric regulation of the active site's conformation. Changes in the active site likely make it less suitable for binding and catalyzing substrate proteins.

Based on the aforementioned hypothesis, five mutations for each one of the three core residues, Val-23', Ile-25', and Ile-29', (a total of 15 peptides) were tested for their capacity to bind to NS3 (Table 1). Four of the amino acids in the synthetic NS4A mutants were bulkier than the corresponding native residues. Two of the bulky mutants were naturally-occurring Phe and Trp, while the other two were unnatural cyclohexylglycine (xG) and homo-isoleucine (hI) (Fig. 1). xG was selected because it is slightly bulkier than isoleucine and valine and has a cyclic conformation. Homo-isoleucine was selected due to its highly flexible side chain, which includes three rotatable bonds whereas xG has only one rotatable bond. Phe and Trp were used as substitutes because they had a markedly larger size than the targeted residues of the native NS4A. The fifth mutation at each targeted position was alanine and was performed to check if previously reported Ala mutants inhibited NS3 after binding or without binding [16].

The binding affinity of NS4A to NS3

First, to determine the binding affinity of these mutants, we established the binding affinity of the native NS4A as a positive reference/control. However, because of the lack of consideration of NS4A as a drug target [20], selection of techniques and experimental conditions had to be resolved before proceeding with the tested synthetic analogs (Pep-1 to Pep-15, Table 1). DSLS was performed since it is a label-free method and, thus, it should be a more appropriate technique for this purpose [35,36].

DSLS evaluates the non-covalent binding of a ligand to a protein by measuring the stability of the protein, expressed as shifts in aggregation temperature (T_{agg}), in the absence and the presence of ligands [36]. In this context, we established optimal conditions for our binding assay first by varying the incubation time, temperature, and protein/peptide ratio. Throughout the process, we adhered to previously reported conditions [37] by mixing NS3 with the synthetic NS4A for 15 min at room temperature. Disappointingly, after repeating the experiment several times and with different batches of protein, it was determined that only weak T_{agg} shifts with high standard error of mean (SEM) were being obtained (Entry 1, Table 2).

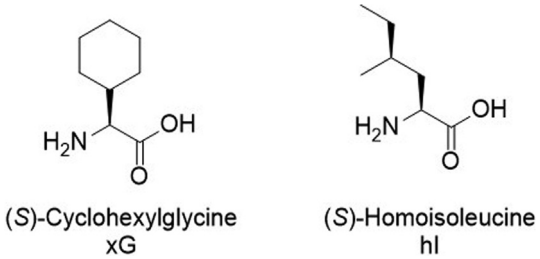

Fig. 1. Structures of xG and hI used as synthetic NS4A analogues.

Table 2
Optimization of the conditions for the DSLS binding affinity tests. The NS3 protein was mixed with NS4A at specified conditions with gentle shaking. The change in stability is expressed as aggregation temperature shifts (ΔT_{agg}) = T_{agg} (NS3) - T_{agg} (NS3 + NS4A).

Entry	Time (min)	Temp. (°C)	Molar ratio (NS4A:NS3)	ΔT_{agg} (°C)	SEM (°C)
1	15	25	1:1	<0.5 (average)	>1.0 (average)
2	30	25	1:1	1.620	0.383
3	60	25	1:1	2.090	0.135
4	120	25	1:1	1.970	0.135
5	120	4	1:1	0.998	0.270
6	30	37	1:1	1.709	0.355
7	90	25	1:2	2.830	0.119
8	30	25	1:2	3.160	0.851

We increased the incubation time to 30 min (Entry 2) and found that the T_{agg} shift increased to 1.6 °C, but the SEM (±0.39 °C) remained unsatisfactory, indicating that more time could be needed for NS4A to assemble completely. After 1 h of binding with NS4A (Entry 3), the aggregation temperature climbed to approximately 2.1 ± 0.13 °C and became stable over the next hour (Entry 4). Changing the temperature (Entries 5 and 6) did not help stabilize the protein further (more details in Supplementary Material, Fig. S5). Reproducibility of the highest T_{agg} shift values, within acceptable standard errors, was obtained by shaking NS3 with NS4A at a 1:2 ratio at room temperature for 2 hrs. Under these conditions, NS3/4A binding resulted in a ΔT_{agg} value of 2.83 ± 0.12 °C (Fig. 2).

To quantify the expression of the binding affinity, we measured the dissociation constant K_d for NS3-NS4A using fluorescence anisotropy. In this method, a fixed amount of FITC-labelled NS4A was mixed with increasing concentrations of unlabeled NS3. Fig. 3A illustrates that 15 min of mixing is insufficient to reach an association/dissociation equilibrium, which is confirmed by the DSLS experiments. Binding of NS4A in our acellular conditions was completed over longer periods of time, and the mixture stayed stable for at least 2 h. The fluorescence anisotropy experiments also determined that the binding affinity of NS4A towards the NS3 enzyme presented a K_d value of 169.3 ± 3.7 nM (1.5 h) under the previously specified conditions (Fig. 3B).

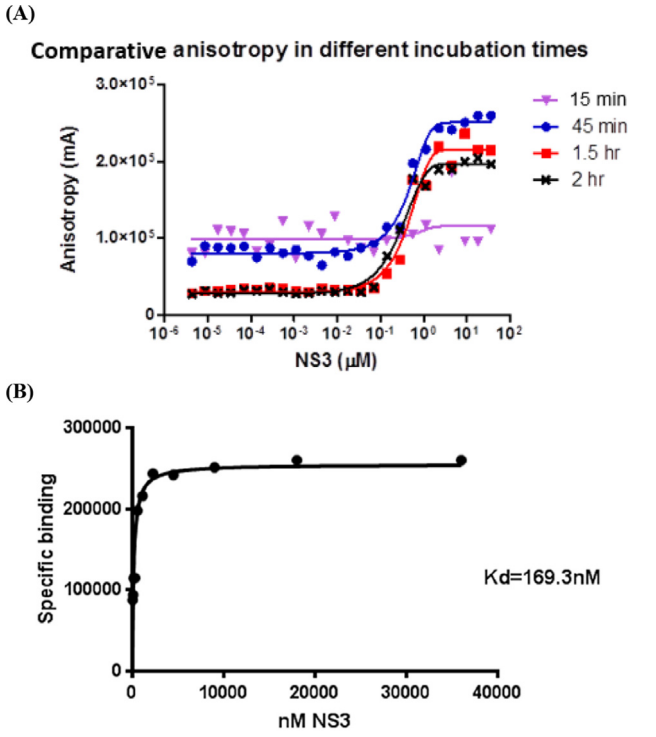

Fig. 3. (A) Fluorescence anisotropy curve of FITC-NS4A (0.1 μM) with NS3 genotype-4 (at different concentrations). Each plot specifies the effect of time on fluorescence. (B) Fluorescence anisotropy plot between variable concentrations of NS3 genotype-4 and 0.1 μM of FITC-$NS4A_{21'-34'}$ core after an incubation period of 90 min. The curve and the dissociation constant was calculated using the single binding site model implemented in GraphPad Prism v.7 software.

The binding affinity of NS4A synthetic analogs

We have taken advantage of the fact that DSLS is a label-free method and used it to measure the relative binding affinity of NS4A synthetic analogs (listed in Table 1) and compared them to the native $NS4A_{21'-34'}$ peptide, in terms of T_{agg} shifts. Results from the DSLS analysis revealed that some of these NS4A mutants could bind to NS3, particularly those with mutations occurring at position Ile-23' (Pep-11 to Pep15), at ratio of 2:1 (Peptide:Protein) (Fig. 4A). The mutant peptide Pep-15 (Val23'-NS4A-xG) exhibited a higher binding affinity than the native peptide in all conditions (see Supplementary Material Fig. S6). The highest T_{agg} shift obtained for Pep-15 was 3.90 °C, which was 1.07 °C higher than that of the native NS4A (2.83 °C) at conditions at 2:1 ratio, room temperature for 2 h) (Fig. 4B).

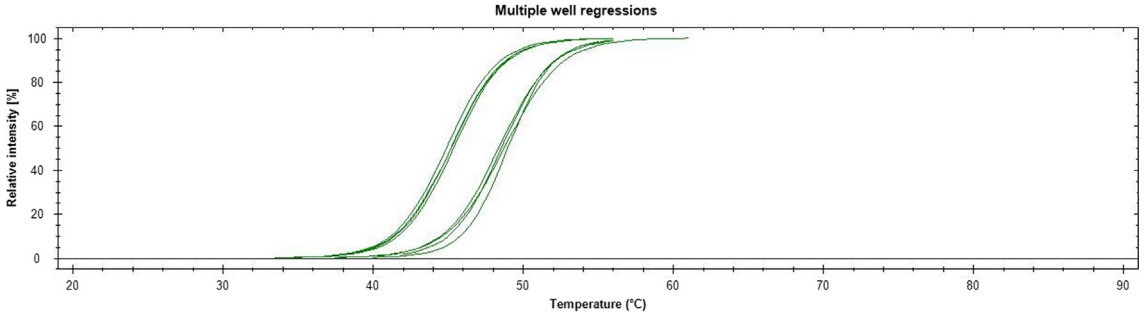

Fig. 2. The DSLS spectrum of HCV genotype-4 NS3 without NS4A (left) and after mixing with native $NS4A_{21'-34'}$ core (KK-GSVVIVGRIVLSG-KK) (right) for 2 h at room temperature with shaking.

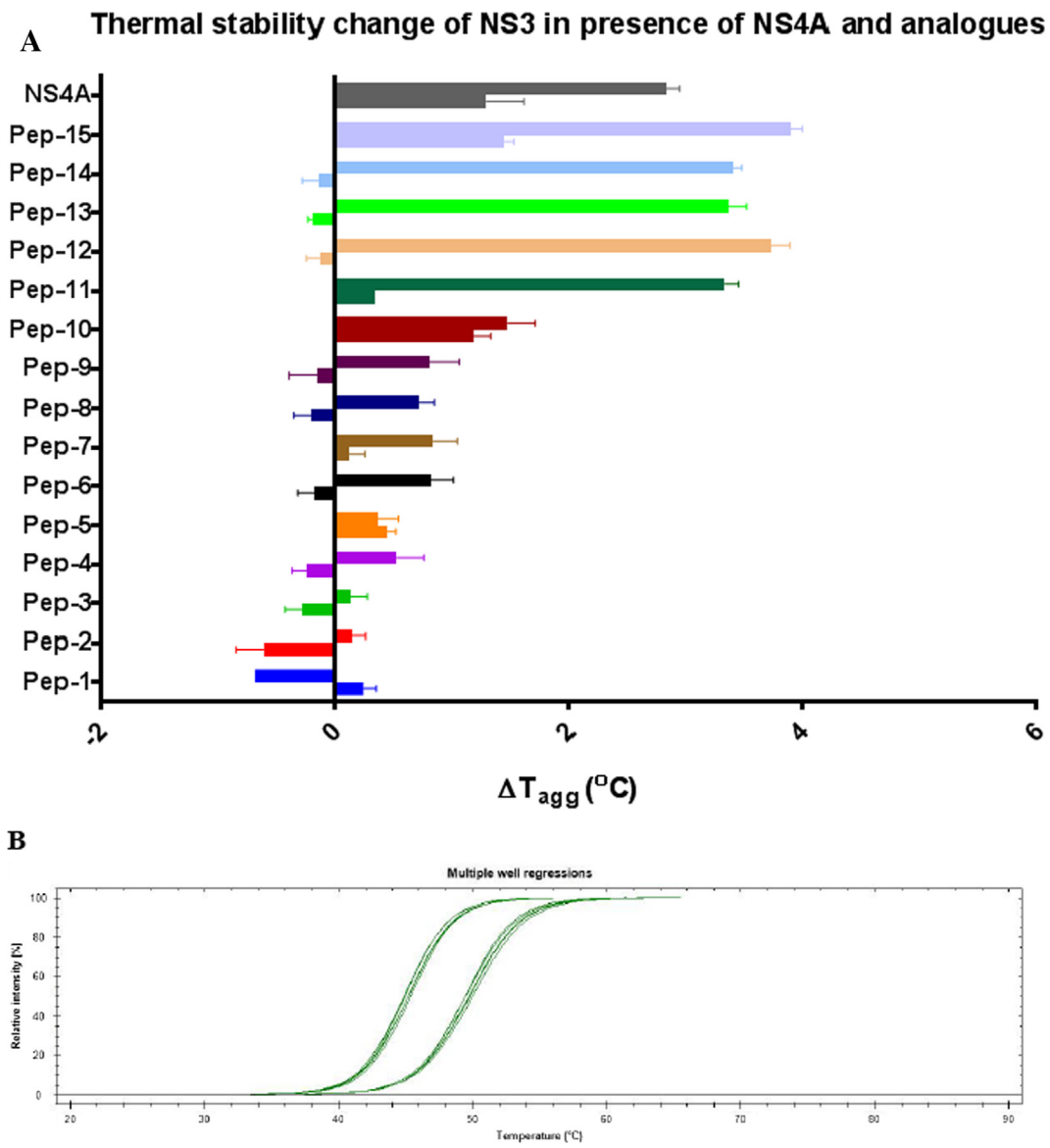

Fig. 4. (A) Changes in the stability of NS3 expressed as differences in aggregation temperature (ΔT_{agg}) ± SEM (see Supplementary Material) when NS3 (15 μM) was mixed with NS4A or its peptide analogs (Pep-1 to Pep-15) and the protein without a cofactor site ligand. Each peptide is colored differently, and stability is expressed in two bars: The bottom bar represents a molar ratio of 1:1 while the top bar represents a molar ratio of 2:1 (Pep:Protein). (B) Aggregation of the NS3 protein under thermal denaturation (DSLS measurement). NS3 alone (left) and a mixture of 15 μM NS3 and 30 μM Pep-15 (right). (For interpretation of the references to colour in this figure legend, the reader is referred to the web version of this article.)

We measured the affinity of Pep-15 using a fluorescence competition assay with FITC-NS4A. In this test, Pep-15 and FITC-$NS4A_{21'-34'}$ were mixed with NS3 at the concentration calculated for equilibrium at the binding constant (0.1 μM and 1.8 μM, respectively); while Pep-15 was added with increasing concentrations, starting from 0.19 μM to 100 μM. The effect of Pep-15 on the fluorescence anisotropy, compared to that of the positive control (mixture without Pep-15 having maximum fluorescence), reflected the level of competition of this peptide for binding to NS4A. The results show that increasing the concentration of Pep-15 produced a concomitant decrease in fluorescence. This was a clear evidence of the ability of Pep-15 to compete with FITC-$NS4A_{21'-34'}$ and replaces it as aNS3 ligand. Using GraphPad Prism 7, The K_d value of Pep-15 was calculated at 70 nM (Fig. 5). It was also noted that the Pep-15 and NS3 complexwas remarkably stable over a significant period of time as indicated by nearly equal fluorescence emissions after 90 and 120 min (Fig. 5, black and red plot curves). Results

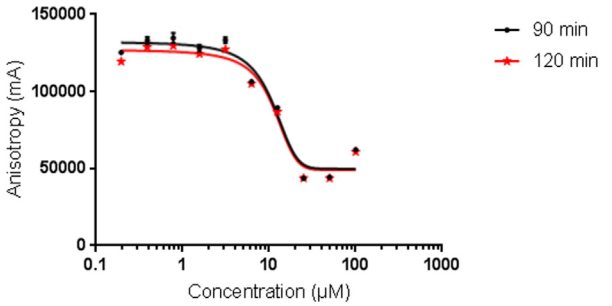

Fig. 5. Fluorescence anisotropy curve of FITC-NS4A/NS3 (0.1/1.8 μM) plotted against varying concentrations of Pep-15.

ofthe fluorescence anisotropy assay was aligned with thermal stabilization tests using DSLS which revealed that Pep-15 binds to NS3 more potently than the native NS4A.

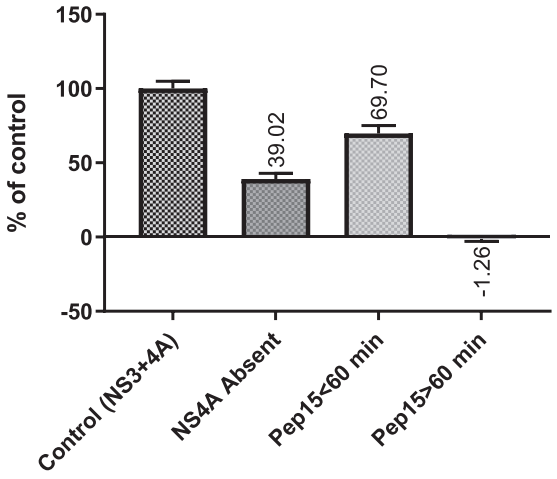

Fig. 6. The catalytic activity of NS3 in the presence or absence of Pep-15. NS3 (4 μM) was mixed with Pep-15 (serial dilution), and then 5-FAM-substrate was added after 15 min. The activity was monitored by measuring fluorescence (excitation 490 nm, emission 520). Fluorescence = Reading-Substrate (in buffer). Control = NS3 + NS4A + Substrate; other columns are NS3 + Buffer + substance specified on each column. The vertical axes (activity % from control) = (fluorescence emission of specified condition/fluorescence emission of control) × 100.

Conclusively, Pep-15, a bulkier Val-23‘ mutant, competes with the native viral peptide and binds to NS3 protease with higher potency.

Enzyme inhibition assay

After confirming the effectiveness with which Pep-15 binds to NS3 by replacing the native NS4A, Pep-15 was tested for its ability to inhibit the protease activity of the NS3 enzyme (Fig. 6). The positive control of this test was provided in the Sensolyte™ kit manual. Thus, if fluorescence was observed after mixing NS3 and NS4A with 5-FAM-substrate, it was considered that these were 100% active (positive control). The NS3 domain (without NS4A) exhibited 39% of the activity obtained from the positive control. Mixing NS3 and Pep-15 (by making 1:2 serial dilutions from 50 μM to 97.6 nM) maintained 69.7% of the enzymatic activity during the first 60 min (fluorescence was measured at intervals of 10 m). After 60 min, it was observed that enzymatic activity completely ceased as compared to the positive control. Even though this experiment was a simple and qualitative test, it provided sufficient evidence to suggest that Pep-15 binds to and forms an inactive complex with NS3. The delayed inhibition of the enzymatic activity observed here coincides with the amount of time (approximately 1 h) required for both NS4A and Pep-15 to intercalate effectively and reach stable complex with NS3 in acellular conditions.

Molecular dynamics (MD) analysis of the impact of Pep-15 binding to NS3

The aim of this modeling study was to investigate possible changes in the active site of NS3 when complexed with Pep-15, instead of native NS4A. Among the many crystal structures of HCV NS3/4A protease present in the protein data bank (PDB), few (e.g. entries 1NS3 [18] and 1A1R [11]) contain the NS4A component as an external synthetic peptide that has been added to an expressed NS3 (non-fusion protein). The vast majority of crystallographic studies utilized NS3/4A constructs as fusion (one strand) proteins because they were focused on discovering substrate site inhibitors for NS3/4A [38–40]. Fortunately, we found that the conformation of NS4A is almost identical amongst the crystal structures present in PDB, regardless of the genotype [38–40] or fusion status [11,18,40] (see Supplementary Material, Fig. S2). When Val-23 was mutated to xG, the new complex was checked visually; nonetheless, no major steric conflicts with any residue around the cyclohexyl group were observed. The shortest distance measured between molecules was 3.2 Å, between the xG side chain and Ala-59. Applying molecular mechanics (energy minimization) did not change the structure of the NS3-Pep15 complex significantly (root mean square deviation, RMSD = 0.29 Å). Most importantly, Pep-15 maintained favorable hydrophobic contact with Phe-43, Leu-64, and Trp-85, which, along with Ala-59, accommodate Val-23 into a well-formed hydrophobic pocket.

A molecular dynamics (MD) analysis was performed to check the stability of this complex for 2 ns. It was observed that the NS3-Pep15 complex reached total energy stability after approximately 0.5 ns (Fig. 7A), but the structure of the complex changed dramatically (RMSD = 3.8 Å).

A visual examination of the pose produced after performing the MD simulation revealed that striking changes occurred following the interaction between the bulkier cyclohexyl group of xG and surrounding hydrophobic residues accommodating the Val-23‘, particularly Ala-59. It was determined that when NS4A intercalates the A_0 and A_1 sheets of NS3, it forms a deep hydrophobic pocket around Val-23‘ (formed of Phe-43, Ala-59, Leu-64, and Trp-85), which reorders Ala-59 and helps the α1-helix (residues Tyr-56 to Gly-60) fold. Subsequently, His-57, an essential member of the catalytic triad, is rearranged resulting in a polar interaction with the second residue in the catalytic triad, Asp-81 (located in F1 β-sheet) [18]. Implementing the MD simulations caused some shift in the conformation of both the Pep-15 xG side chain and the hydrophobic residues around it (Fig. 7C). A crucial trajectory in our MD simulation was the motility of Ala-59, where a 3.5 Å shift was observed. Regardless of the number of shifts occurring in all residues (Fig. 7C), this hydrophobic pocket did not collapse, and the cyclohexyl side chain of xG maintained its presence as well as interactions within this hydrophobic pocket after the MD simulation (Fig. 7C). However, the shift in Ala-59 brought changes to the catalytic triad, particularly in Ser-139. This residue lies in a flexible loop connecting α2-helix and D2-sheet. After 2.0 ns of MD simulations at 310 °K, Ser-139 was obviously shifted safrom its catalytic triad companions, His-57 and ASP-81, by 5.9 Å, thus losing interaction with them. It was surprising that His-57 and its imidazole ring shifted only1.6 Å while its imidazole ring shifted 0.8 Å repecitvely. Therefore, the MD simulations suggest that the xG mutation does not disrupt the ionic interaction between His-57 and Asp-81; nonetheless, it damaged the catalytic apparatus of the NS3 enzyme (Fig. 7B). The MD experiments, in our view, furnished insight on how and why Pep-15 binds to HCV-NS3 to form an inactive complex.

Conclusion

Validating NS4A competitors as a new concept for development of efficient antiviral agents has been suggested in 1990s upon the characterization on NS3/4A protease as a target for development of HCV agents, but it has largely under explored. The question remained for more than two decades whether ligands of NS4A binding pocket will inhibit the function of NS4A. The answer of this question has been settled in this work using a series of bulkier mutants of $NS4A_{21'-34'}$. We identified Val-23‘-$NS4A_{21'-34'}$-xG (Pep-15) as a bulkier mutant that bind to NS4A site and inhibit the HCV-NS3 catalytic function by forming an inactive complex. Regardless of whether Pep-15 can be considered a drug candidate, this accomplishment encourages more research towards discovering new classes of potent HCV NS3 protease inhibitors. It also set

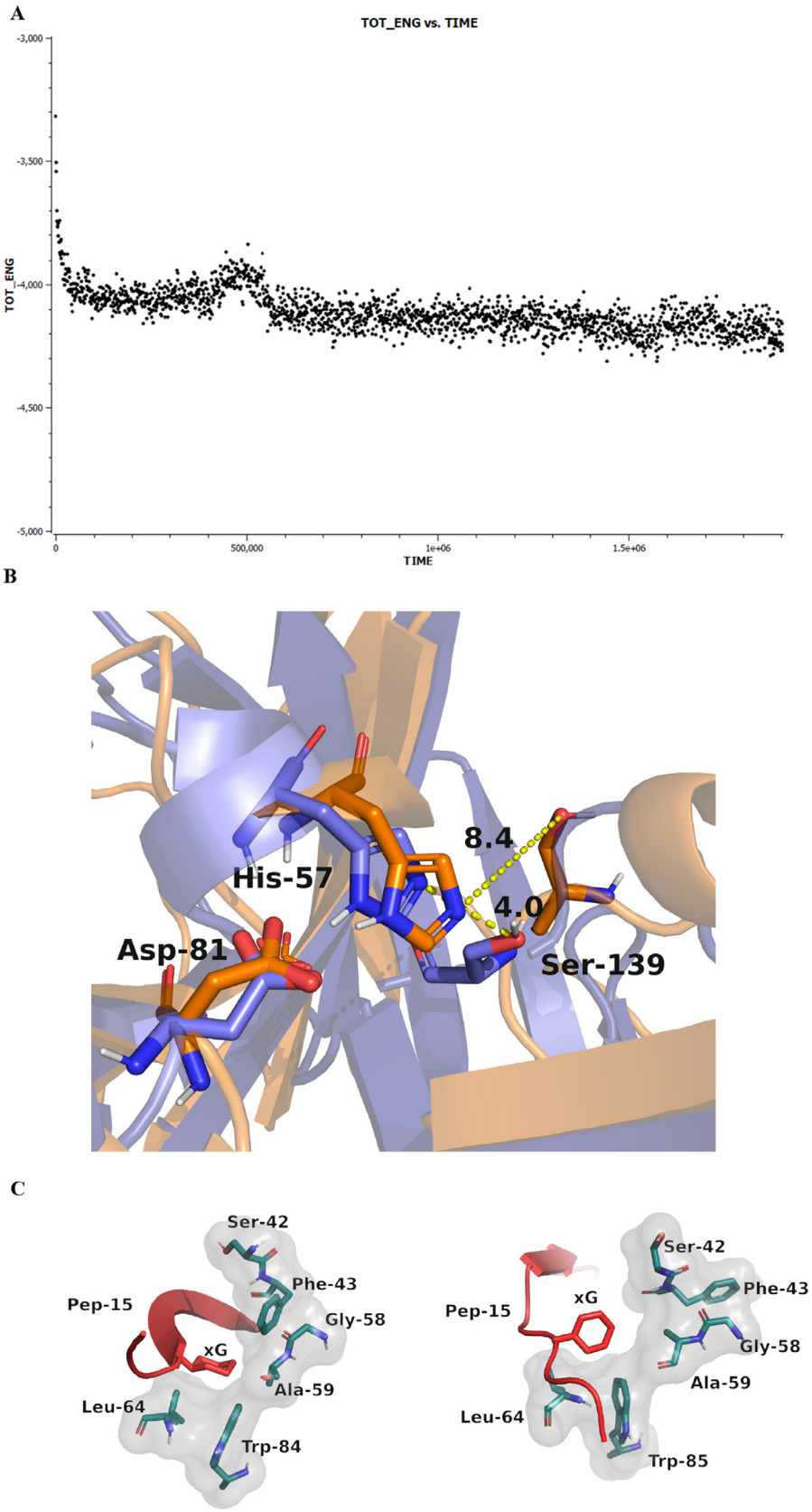

Fig. 7. Molecular Dynamics (MD) simulation of Pep-15 created by mutating Val-23 in the crystal structure PDB Code: 1NS3 [18]. (A) A plot of total energy for 0.0 to 2.0 ns. (B) Comparison of the catalytic triad positions before (blue) and after (orange) molecular dynamics simulations. Note the minimal motility of Asp81 and His57. The striking motion (8.4 Å) of Ser139 leads to the loss of hydrogen bonding. (C) The change in the hydrophobic pocket (around xG) from its initial structure (0.0 ns) (left) and final trajectory (2.0 ns) (right). The residues contributing to the pocket occurred on the solvent-excluded (Connolly) surface. NS3 residues are colored in green while Pep-15 is colored in red. (For interpretation of the references to colour in this figure legend, the reader is referred to the web version of this article.)

forth a future strategy to design non-peptide mimics of NS4A, which is currently undergoing and will be published elsewhere. Future research could have far-reaching effects since NS4A is a common factor in the *Flaviviridae* family of viruses.

Compliance with Ethical Requirements

This article does not contain any studies with human or animal subjects.

Acknowledgments

This project was funded by the National Plan for Science, Technology and Innovation (MAARIFAH), King Abdulaziz City for Science and Technology, the Kingdom of Saudi Arabia; Award number 12-BIO3193-03. The authors also, acknowledge with thanks Science and Technology Unit, King Abdulaziz University for technical support. The research by STA reported in this publication was supported by funding from King Abdullah University of Science and Technology (KAUST).

Declaration of Competing Interest

The authors have declared no conflict of interest.

Appendix A. Supplementary material

Supplementary data to this article can be found online at https://doi.org/10.1016/j.jare.2020.01.003.

References

[1] Guzman H, Contreras-Gutierrez MA, Travassos da Rosa APA, Nunes MRT, Cardoso JF, Popov VL, et al. Characterization of three new insect-specific flaviviruses: their relationship to the mosquito-borne flavivirus pathogens. Am J Trop Med Hyg 2018;98(2):410–9.
[2] Richard AS, Shim BS, Kwon YC, Zhang R, Otsuka Y, Schmitt K, et al. AXL-dependent infection of human fetal endothelial cells distinguishes Zika virus from other pathogenic flaviviruses. Proc Natl Acad Sci USA 2017;114(8):2024–9.
[3] Simmonds P, Becher P, Bukh J, Gould EA, Meyers G, Monath T, et al. ICTV virus taxonomy profile: flaviviridae. J Gen Virol 2017;98(1):2–3.
[4] Murray CL, Jones CT, Rice CM. Architects of assembly: roles of Flaviviridae non-structural proteins in virion morphogenesis. Nat Rev Microbiol 2008;6(9):699–708.
[5] Tanji Y, Hijikata M, Satoh S, Kaneko T, Shimotohno K. Hepatitis C virus-encoded nonstructural protein NS4A has versatile functions in viral protein processing. J Virol 1995;69(3):1575–81.
[6] Ishido S, Fujita T, Hotta H. Complex formation of NS5B with NS3 and NS4A proteins of hepatitis C virus. Biochem Biophys Res Commun 1998;244(1):35–40.
[7] Kim DW, Gwack Y, Han JH, Choe J. C-terminal domain of the hepatitis C virus NS3 protein contains an RNA helicase activity. Biochem Biophys Res Commun 1995;215(1):160–6.
[8] Wölk B, Sansonno D, Kräusslich H-G, Dammacco F, Rice CM, Blum HE, et al. Subcellular localization, stability, and trans-cleavage competence of the hepatitis C virus NS3-NS4A complex expressed in tetracycline-regulated cell lines. J Virol 2000;74(5):2293–304.
[9] Li K, Foy E, Ferreon JC, Nakamura M, Ferreon AC, Ikeda M, et al. Immune evasion by hepatitis C virus NS3/4A protease-mediated cleavage of the Toll-like receptor 3 adaptor protein TRIF. Proc Natl Acad Sci USA 2005;102(8):2992–7.
[10] Meylan E, Curran J, Hofmann K, Moradpour D, Binder M, Bartenschlager R, et al. Cardif is an adaptor protein in the RIG-I antiviral pathway and is targeted by hepatitis C virus. Nature 2005;437(7062):1167.
[11] Kim J, Morgenstern K, Lin C, Fox T, Dwyer M, Landro J, et al. Crystal structure of the hepatitis C virus NS3 protease domain complexed with a synthetic NS4A cofactor peptide. Cell 1996;87(2):343–55.
[12] Failla C, Tomei L, De Francesco R. Both NS3 and NS4A are required for proteolytic processing of hepatitis C virus nonstructural proteins. J Virol 1994;68(6):3753–60.
[13] Love RA, Parge HE, Wickersham JA, Hostomsky Z, Habuka N, Moomaw EW, et al. The conformation of hepatitis C virus NS3 proteinase with and without NS4A: a structural basis for the activation of the enzyme by its cofactor. Clin Diagn Virol 1998;10(2):151–6.
[14] Butkiewicz NJ, Wendel M, Zhang R, Jubin R, Pichardo J, Smith EB, et al. Enhancement of hepatitis C virus NS3 proteinase activity by association with NS4A-specific synthetic peptides: identification of sequence and critical residues of NS4A for the cofactor activity. Virology 1996;225(2):328–38.
[15] Lin C, Thomson JA, Rice CM. A central region in the hepatitis C virus NS4A protein allows formation of an active NS3-NS4A serine proteinase complex in vivo and in vitro. J Virol 1995;69(7):4373–80.
[16] Shimizu Y, Yamaji K, Masuho Y, Yokota T, Inoue H, Sudo K, et al. Identification of the sequence on NS4A required for enhanced cleavage of the NS5A/5B site by hepatitis C virus NS3 protease. J Virol 1996;70(1):127–32.
[17] Tomei L, Failla C, Vitale RL, Bianchi E, De Francesco R. A central hydrophobic domain of the hepatitis C virus NS4A protein is necessary and sufficient for the activation of the NS3 protease. J Gen Virol 1996;77(5):1065–70.
[18] Yan Y, Li Y, Munshi S, Sardana V, Cole JL, Sardana M, et al. Complex of NS3 protease and NS4A peptide of BK strain hepatitis C virus: a 2.2 A resolution structure in a hexagonal crystal form. Prot Sci 1998;7(4):837–47.
[19] Hamad HA, Thurston J, Teague T, Ackad E, Yousef MS. The NS4A cofactor dependent enhancement of HCV NS3 protease activity correlates with a 4D geometrical measure of the catalytic triad region. PLoS ONE 2016;11(12):e0168002.
[20] De Francesco R, Pessi A, Steinkühler C. Mechanisms of hepatitis C virus NS3 proteinase inhibitors. J Viral Hepatitis 1999;6:23–30.
[21] Kiser JJ, Flexner C. Direct-acting antiviral agents for Hepatitis C virus infection. Annu Rev Pharmacol Toxicol. 2013;53(1):427–49.
[22] Portal-Núñez S, González-Navarro CJ, García-Delgado M, Vizmanos JL, Lasarte JJ, Borrás-Cuesta F. Peptide inhibitors of Hepatitis C virus NS3 protease. Antiviral Chem Chemother 2003;14(5):225–33.
[23] Attwood MR, Bennett JM, Campbell AD, Canning GG, Carr MG, Conway E, et al. The design and synthesis of potent inhibitors of hepatitis C virus NS3-4A proteinase. Antivir Chem Chemother 1999;10(5):259–73.
[24] Llinas-Brunet M, Bailey M, Fazal G, Goulet S, Halmos T, Laplante S, et al. Peptide-based inhibitors of the hepatitis C virus serine protease. Bioorg Med Chem Lett 1998;8(13):1713–8.
[25] Llinàs-Brunet M, White PW. Discovery and Development of BILN 2061 and Follow-Up BI 201335. In: Kazmierski WM, editor. Antiviral drugs. Hoboken, NJ: John Wiley & Sons; 2011. p. 225–38.
[26] Massariol M-J, Zhao S, Marquis M, Thibeault D, White PW. Protease and helicase activities of hepatitis C virus genotype 4, 5, and 6 NS3–NS4A proteins. Biochem Biophys Res Commun 2010;391(1):692–7.
[27] Mohamoud YA, Riome S, Abu-Raddad LJ. Epidemiology of hepatitis C virus in the Arabian Gulf countries: Systematic review and meta-analysis of prevalence. Int J Infect Dis 2016;46:116–25.
[28] Gomaa A, Allam N, Elsharkway A, El Kassas M, Waked I. Hepatitis C infection in Egypt: prevalence, impact and management strategies. Hepat Med 2017;9:17–25.
[29] Vedadi M, Niesen FH, Allali-Hassani A, Fedorov OY, Finerty Jr PJ, Wasney GA, et al. Chemical screening methods to identify ligands that promote protein stability, protein crystallization, and structure determination. Proc Natl Acad Sci USA 2006;103(43):15835–40.
[30] Hamill P, Jean F. Enzymatic characterization of membrane-associated Hepatitis C Virus NS3-4A Heterocomplex serine protease activity expressed in human cells. Biochemistry 2005;44(17):6586–96.
[31] Case DA, Cheatham 3rd TE, Darden T, Gohlke H, Luo R, Merz Jr KM, et al. The Amber biomolecular simulation programs. J Comput Chem 2005;26(16):1668–88.
[32] Love RA, Parge HE, Wickersham JA, Hostomsky Z, Habuka N, Moomaw EW, et al. The crystal structure of hepatitis C virus NS3 proteinase reveals a trypsin-like fold and a structural zinc binding site. Cell 1996;87(2):331–42.
[33] Hagel M, Niu D, St Martin T, Sheets MP, Qiao L, Bernard H, et al. Selective irreversible inhibition of a protease by targeting a noncatalytic cysteine. Nat Chem Biol 2011;7(1):22.
[34] Prongay AJ, Guo Z, Yao N, Pichardo J, Fischmann T, Strickland C, et al. Discovery of the HCV NS3/4A Protease Inhibitor (1R,5S)-N-[3-Amino-1-(cyclobutylmethyl)-2,3-dioxopropyl]-3-[2(S)-[[[(1,1-dimethylethyl)amino]carbonyl]amino]-3,3-dimethyl-1-oxobutyl]-6,6-dimethyl-3-azabicyclo[3.1.0]hexan-2(S)-carboxamide (Sch 503034) II. Key Steps in Structure-Based Optimization. J Med Chem 2007;50(10):2310–8.
[35] Hameed US, Haider I, Jamil M, Kountche BA, Guo X, Zarban RA, et al. Structural basis for specific inhibition of the highly sensitive ShHTL7 receptor. EMBO Rep 2018;19(9):e45619.
[36] Senisterra GA, Markin E, Yamazaki K, Hui R, Vedadi M, Awrey DE. Screening for ligands using a generic and high-throughput light-scattering-based assay. J Biomol Screen 2006;11(8):940–8.
[37] Thibeault D, Bousquet C, Gingras R, Lagacé L, Maurice R, White PW, et al. Sensitivity of NS3 serine proteases from hepatitis C virus genotypes 2 and 3 to the inhibitor BILN 2061. J Virol 2004;78(14):7352–9.
[38] Soumana DI, Kurt Yilmaz N, Ali A, Prachanronarong KL, Schiffer CA. Molecular and dynamic mechanism underlying drug resistance in genotype 3 Hepatitis C NS3/4A Protease. J Am Chem Soc 2016;138(36):11850–9.
[39] Jiang Y, Andrews SW, Condroski KR, Buckman B, Serebryany V, Wenglowsky S, et al. Discovery of Danoprevir (ITMN-191/R7227), a highly selective and potent inhibitor of Hepatitis C Virus (HCV) NS3/4A Protease. J Med Chem 2014;57(5):1753–69.
[40] Taylor JG, Zipfel S, Ramey K, Vivian R, Schrier A, Karki KK, et al. Discovery of the pan-genotypic hepatitis C virus NS3/4A protease inhibitor voxilaprevir (GS-9857): a component of Vosevi®. Bioorg Med Chem Lett 2019;29(16):2428–36.